

Dynamical Trajectory Replanning for Uncertain Environments

Shai Revzen*

B. Deniz İlhan*

Daniel E. Koditschek*

Abstract—We propose a dynamical reference generator equipped with an augmented transient “replanning” subsystem that modulates a feedback controller’s efforts to force a mechanical plant to track the reference signal. The replanner alters the reference generator’s output in the face of unanticipated disturbances that drive up the tracking error. We demonstrate that the new reference generator cannot destabilize the tracker, that tracking errors converge in the absence of disturbance, and that the overall coupled reference-tracker system cannot be destabilized by disturbances of bounded energy. We report the results of simulation studies exploring the performance of this new design applied to a two dimensional point mass particle interacting with fixed but unknown terrain obstacles.

I. INTRODUCTION

Over the past two decades, the field of robotics has given rise to many examples of notional [1–4] and arguably [5] or potentially [6, 7] useful working physical machines whose behavioral goals are encoded by means of reference dynamics rather than the more traditional reference trajectory. In this paper we pursue a general framework for stably coupling dynamical reference generators to actuated mechanical systems last addressed in such abstracted (rather than robot-specific) form more than two decades ago [8].

We study the tracking problem for a fully actuated, force-controlled, unit-mass point-mechanism with configuration space $\mathcal{Q} := \mathbb{R}^n$ subject to a force disturbance d ,

$$\ddot{q} = Q[q; r] + d, \quad (1)$$

where Q denotes a causal functional of the trajectory of the plant q and of a desired reference motion path r . Because physical actuators suffer severe limitations we restrict attention to designs for which both the force input (the output of Q) and the rate of mechanical work (omitting work done by the disturbance) are bounded.

In the traditional robotics and control paradigm [9] some “higher level” planner generates a sufficiently smooth¹ reference trajectory $r : \mathbb{R} \rightarrow \mathcal{Q}$ that encodes the task at hand. The presumably task-naive but tracking-expert controller produces forces excited by the augmented tracking error, $Q[q; r] := \ddot{r} - E[e, \dot{e}]$ where $e := r - q \in \mathcal{Q}$ and E is a force law chosen so that the resulting tracking error system

$$\ddot{e} = E(e, \dot{e}) - d \quad (2)$$

converges as strongly as possible to zero despite disturbances d . Within the controls field, one counterpart to our work

is the longstanding anti-windup literature [11] wherein the unexecutably high authority commands of some nominal tracking controller are trimmed back to respect the saturating nature of inputs to the plant (1), and the very active reference governor literature [12] provides controllers which do so with formal convergence guarantees. Indeed, any of the variants on these constructions which yield iISS [13] closed loops (2) with guaranteed Lyapunov functions [14], suitable for second order systems [15] would be appropriate candidates to generate the posited error tracker (2), although for purposes of illustration in this paper we use a very much simpler saturating potential-dissipative [16] tracker (21).

In contrast, the focus of this paper is the question of what benefit can be achieved by modifying the reference trajectory r in the face of online exposure to the disturbances d . Specifically, we advance an architecture relevant to the growing class of robots [1–6] whose reference trajectories are dynamically generated by allowing disturbance induced tracking errors (2) to excite a transient “replanner” subsystem that alters the reference generator in a stable manner.

The inevitable inaccuracies in world model, sensor acuity and actuator fidelity represented by d in (1) usually have a systematic (albeit unmodeled) as well as a random component and we believe that such recourse to simple *dynamical replanning* may allow the plant to avoid rather than fight against otherwise intransigent if not adversarial obstacles.

After presenting the formal scheme we demonstrate our ideas for the class of dynamical trajectory replanning problems generated by fixed, unforeseen obstacles in the configuration space \mathcal{Q} that can be modeled by disturbances, d , taking the form of time invariant repelling potential fields (the known structure) whose specific functional form is not available (the uncharacterized detail). Our formal results are limited to the demonstration that the proposed construction does not destabilize the tracker (i.e. the transient-augmented reference generator is ISS [13, 17]), that the system will converge in absence of a disturbance (i.e., the complete closed loop generator-tracker system is 0-GAS), and that the system does not destabilize for disturbance inputs with bounded energy (system is iISS [18]), notwithstanding our present inability to predict which classes of obstacles will be successfully eluded by the replanner and thus generate only bounded energy disturbance signals.

Section II introduces some previous work and ideas on which the present results depend. Section III lays out the proposed new controller design starting from some reference dynamics f and dynamically generated recovery maneuvers g . The section proves the ISS, 0-GAS and iISS properties of the relevant subsystems with respect to a (presumed compact)

* Electrical and Systems Engineering Department, University of Pennsylvania, 200 S. 33rd St. Moore 203, Philadelphia, PA 19104, USA {shrevzen, bdeniz, kod}@seas.upenn.edu

¹ In this paper it is convenient to assume that all our signals are C^∞ , but physical actuators are generally adequately protected from long term mechanical (albeit not necessarily thermal [10]) harm by C^2 inputs.

goal set. In Section IV we report the results of simulated examples of our controller applied to two dimensional plants interacting with fixed, but unknown terrain obstacles.

II. BACKGROUND IDEAS AND DESIGN

In this section we present the conceptual geometric ideas that lead us to our design. The equations in this section are not used in our main result. Instead, they are intended to serve the reader with a rationale for the more elaborate constructions that follow.

A. A First Order Graph as a Second Order Attractor

Following [8], we assume a given geometrically defined task [19] encoded as a smooth first order reference dynamical system,

$$\dot{r} = f(r), \quad (3)$$

endowed with a known Lyapunov function ϕ_r . Examples of nontrivial geometrically defined tasks that are nicely amenable to second order lifts of first order dynamical encodings are obstacle avoidance problems [8, 20], group formation coordination [21], and even complex kinodynamic motion planning problems [22, 23]. Define the second order “lift”

$$\ddot{r} = R_{(f, \phi_r)}(r, \dot{r}) := \dot{f} - \kappa_r[\dot{r} - f(r)] - \nabla \phi_r r \quad (4)$$

where $\dot{f} := D_r f(r)\dot{r}$, $\nabla \phi_r r := [D_r \phi_r]^T$. Observe [8] $\eta_r := \phi_r + \frac{1}{2}|\dot{r} - f(r)|^2$ is a Lyapunov function for (4).

In the next section we will replace (4) with an augmented construction (8),(9) that accepts the replanner’s transient inputs, respecting which appropriate assumptions on ϕ_r insure that η_r is an ISS-Lyapunov function as well.

B. Internal Dynamical Reference Generators

Although there can be great virtue in self-excited designs wherein a copy of (3) is placed directly in the plant’s feedback path (e.g. [1–4]) this paper focuses on a control scheme that places the reference dynamics in the feedforward pathway using a design akin to

$$\begin{aligned} \ddot{r} &= R(r, \dot{r}) + u(e) \\ \dot{q} &= \dot{r} - E(e, \dot{e}) + d \end{aligned} \quad (5)$$

For example, the original RHex [5] controller adopted a completely open loop version (i.e., with $u \equiv 0$) of this architecture on the torus, $\mathcal{Q} \approx \mathbb{T}^N$. A compensating feedback term was added and tuned to achieve better performance subsequently in RHex [24], and has proven essential to the RiSE climbing machine [7]. The lift in (5) of the reference dynamics (3) now constitutes an internal model – a separate “imagined” copy of q representing the desired plant state and future trajectory – whose value we seek to exploit in recognizing situations of “surprise” and replanning in response.

Toward that end, we now proceed to develop a controller design recipe that augments this internal model with a “maneuver generator / replanner,” s , governed by a smooth time-invariant vector field, g , over some Euclidean space,

\mathcal{S} . This replanner excites the reference dynamics to express recovery maneuvers when an error builds up.

A consequence of “physical” restrictions is that the system cannot reject all bounded disturbances, since adversarial or even blind disturbances larger than the system’s force and power budget can always disrupt any controller’s attempts at correction. Instead, a more subtle notion of stability is needed – the notion of “Integral Input to State Stability (iISS)” [13, 18] – which relates the L_2 norm of the disturbance to a (L_∞) bound on the state of the controller. We make additional use of control-theoretic tools from the “Input to State Stability (ISS)”[17] toolbox in demonstrating that our cascaded design has a response to the disturbance that is guaranteed to be bounded, and which will ultimately converge to the desired motion if the disturbance ceases. In the context of persistent state-dependent disturbances such as the unknown terrain obstacles in our examples, the disturbance ceases whenever the system manages to bypass these obstacles – and thus we are guaranteed that should it succeed in escaping entrapment, the system will resume correct behavior. Notice that trajectories generated through this design recipe are not optimal in any sense. We merely guarantee that the replanner implements a feasible course of action in the face of arbitrary disturbances while respecting force and power limitations.

III. CONTROLLER DESIGN

Denote the zero section over any submanifold $\mathcal{X} \subseteq \mathcal{Q}$ as $\mathcal{Z}_{\mathcal{X}} := \{(q, 0) \in \text{T}\mathcal{Q} | q \in \mathcal{X}\}$.

Assume the following design requirements from the component dynamical systems:

- (1) A fully actuated, unit mass, second order plant with state $(q, \dot{q}) \in \text{T}\mathcal{Q}$.
- (2) A task encoded as a first order dynamical control system

$$\dot{r} = f(r) + v(r, s) \quad (6)$$

over $r \in \mathcal{R} \subseteq \mathcal{Q}$, with input $s \in \mathcal{S}$.

- (2a) (6) is ISS with respect to some compact attractor \mathcal{G}_r and the input s .
- (2b) The coupling term $v(r, s)$ is monotonically bounded in $|s|_{\mathcal{G}_s}$ with respect to a \mathcal{K}_∞ comparison function $\nu(\cdot)$: $|v(r, s)| < \nu(|s|_{\mathcal{G}_s})$
- (2c) The task admits ϕ_r , a smooth ISS-Lyapunov function (in the sense of [25] section 2.1) which also has a saturating gradient. Namely, there exists some $F_{max} \in \mathbb{R}_{>0}$ such that $|\nabla \phi_r(r)| \leq F_{max}$
- (2d) The replanner excitation function $u : \mathcal{Q} \rightarrow \text{TS}$ is zero at zero, globally bounded $\|u(e)\| < u_{max}$ and continuous everywhere except perhaps at zero.
- (3) A replanner encoded as a first order dynamical control system $\dot{s} = g(s) + u$ which is ISS with respect to some compact attractor \mathcal{G}_s and the input u .
- (4) A tracker system $\dot{e} = E(e, \dot{e}) + d$ which is iISS with respect to the point attractor \mathcal{Z}_0 and the input d .

Using these components, selecting a gain $\kappa_r \in \mathbb{R}_{>0}$, and defining $e := r - q \in \mathcal{Q}$, we propose a control system in the

following form:

$$\dot{s} = g(s) + u(e) \quad (7)$$

$$\dot{w} = -\kappa_r w - \nabla \phi_r(r) \quad (8)$$

$$\dot{r} = w + f(r) + v(r, s) \quad (9)$$

$$\ddot{q} = \ddot{r} - E(e, \dot{e}) - d \quad (10)$$

$$\ddot{e} = E(e, \dot{e}) + d \quad (10')$$

Our key theoretical result is expressed as follows:

Theorem 1: The proposed architecture (7)-(10), possesses the following stability properties:

[iISS] The combined dynamics of (e, \dot{e}, r, w, s) is iISS with respect to input d and the attractor \mathcal{A} where $\mathcal{A} := \mathcal{Z}_0 \times \mathcal{Z}_{\mathcal{G}_r} \times \{0\}$. \mathcal{A} is an attracting invariant submanifold of the unforced system (i.e. $d \equiv 0$).

[ISS] The projection of the system to (r, w, s) is ISS with respect to the attractor $\mathcal{Z}_{\mathcal{G}_r} \times \{0\}$ and the input e .

[BP] The undisturbed ($d \equiv 0$) input to the mechanical plant (10) is bounded as is its internal mechanical power.

Note that for the range of intended applications the disturbance will be (in part) state dependent and we have not yet established any useful sufficient conditions (e.g., properties of the replanner relative to the obstacles' shapes and placements) guaranteeing that the disturbance will have bounded energy (e.g., that the replanner will succeed in eluding those obstacles). The theorem merely guarantees the replanner will not itself destabilize the internal reference and mechanical plant dynamics assuming the disturbance desists.

Proof: The proof that follows relies strongly on various properties of ISS systems and iISS systems; see [13] for an excellent tutorial overview of these ideas.

Given Proposition 2 below, we conclude that the second order system (8), (9) is ISS with respect to its input s . The system (7) was assumed to be ISS with respect to its attractor \mathcal{G}_r and the input u . The (compact-set)-ISS property is preserved by cascade composition, thus (7) into (8) into (9) is ISS with respect to the input u , proving [ISS].

Because u is bounded by construction, and the ISS property implies "Bounded Input to Bounded State (BIBS)", [ISS] also proves that (r, w, s) are bounded, and thus [BP] is proven via (10).

As per design requirement (4), (10') is iISS. From proposition 2 of [26], cascade of an iISS system into an ISS system is also iISS proving that cascading (10') into (7), (8) and (9) is iISS and establishing [iISS]. ■

Proposition 2: The system $(r, w) \in \text{TR}$ from (8), (9) is ISS with respect to input s and compact attractor $\mathcal{Z}_{\mathcal{G}_r}$.

Proof: The zero section $\mathcal{Z}_{\mathcal{G}_r}$ is compact from the previously assumed compactness of \mathcal{G}_r . Sontag and Wang [25] section 2.1 provide two equivalent definitions for an "ISS-Lyapunov function" $V : \mathbb{R}^n \rightarrow \mathbb{R}_{\geq 0}$ whose existence with respect to some compact goal set $\mathcal{H} \subseteq \mathbb{R}^n$ is equivalent to the ISS property with respect to \mathcal{H} . V must be proper and positive definite with respect to \mathcal{H} , and there must exist "comparison functions" $\alpha_1, \alpha_2, \chi \in \mathcal{K}_\infty$ such that for all

$\xi \in \mathbb{R}^n$:

$$\alpha_1(|\xi|_{\mathcal{H}}) \leq V(\xi) \leq \alpha_2(|\xi|_{\mathcal{H}}) \quad ([25] \text{ eqn. } 5)$$

$$\xi \neq 0 \wedge |\xi|_{\mathcal{H}} \geq \chi(|v|) \Rightarrow \dot{V}(\xi) < 0 \quad ([25] \text{ eqn. } 8)$$

We proceed to show that $\eta_r(r, w) := \frac{1}{2}w^2 + \phi_r(r)$ is an ISS-Lyapunov function.

From the assumption that $\phi_r(r)$ is ISS-Lyapunov we conclude that it is smooth, proper, positive, and vanishes precisely on the set \mathcal{G}_r , and thus η_r is also smooth, proper, positive and vanishes precisely on the set $\mathcal{Z}_{\mathcal{G}_r}$. Now taking the Lie derivative of ϕ_r along the motions of system (8), (9) we have

$$\dot{\eta}_r = \dot{w} \cdot w + \nabla \phi_r \cdot \dot{r} = -\kappa_r |w|^2 + \nabla \phi_r \cdot (f + v) \quad (11)$$

From [25] eqn. (8) applied to ϕ_r , we conclude the existence of a comparison function $\chi \in \mathcal{K}_\infty$ that satisfies

$$|r|_{\mathcal{G}_r} > \chi(|s|_{\mathcal{G}_s}) \Rightarrow \nabla \phi_r(r) \cdot (f + v) < 0. \quad (12)$$

As an ISS-Lyapunov function with respect to input v , ϕ_r is also perforce a Lyapunov function for the zero input system $\dot{r} = f(r)$, and we conclude $\nabla \phi_r \cdot f \leq 0$ everywhere except \mathcal{G}_r .

With these observations in hand, we define a comparison function $\beta(\cdot)$

$$\beta^2(x) := (F_{max}/\kappa_r)\nu(x) + \chi^2(x), \quad (13)$$

and note that $\nu, \chi \in \mathcal{K}_\infty$ ensure $\beta \in \mathcal{K}_\infty$.

We wish to show that $|r, w|_{\mathcal{Z}_{\mathcal{G}_r}} > \beta(|s|_{\mathcal{G}_s})$ implies $\dot{\eta}_r < 0$, and so as to satisfy [25] eqn. (8). Consider two cases: $|r|_{\mathcal{G}_r} > \chi(|s|_{\mathcal{G}_s})$ and its complement. In the first case, because the term $-\kappa_r |w|^2$ in (11) is negative definite we have $\nabla \phi_r(r) \cdot (f + v) < 0$ from (12) and therefore $\dot{\eta}_r < 0$ is satisfied.

It remains to handle the complementary case $|r|_{\mathcal{G}_r} \leq \chi(|s|_{\mathcal{G}_s})$. By definition, $|r, w|_{\mathcal{Z}_{\mathcal{G}_r}}^2 := |w|^2 + |r|_{\mathcal{G}_r}^2$, motivating the derivation

$$\begin{aligned} |r, w|_{\mathcal{Z}_{\mathcal{G}_r}}^2 &= |w|^2 + |r|_{\mathcal{G}_r}^2 > \beta^2(|s|_{\mathcal{G}_s}) \\ |w|^2 &> \beta^2(|s|_{\mathcal{G}_s}) - \chi^2(|s|_{\mathcal{G}_s}), \end{aligned}$$

with the last step using the assumption of this case. Substituting from (13), obtain

$$\kappa_r |w|^2 > F_{max}\nu(x) > |\nabla \phi_r(r)| \cdot |v(r, s)| \quad (14)$$

$$> \nabla \phi_r(r) \cdot v(r, s) + \nabla \phi_r \cdot f(r) \quad (15)$$

with the (14) from design requirements (2b) and (2c); and (15) from $\nabla \phi_r \cdot f \leq 0$.

From (15), we see that in both cases considered the RHS of (11) is negative definite with respect to the compact set $\mathcal{Z}_{\mathcal{G}_r}$. This RHS vanishes only on $\mathcal{Z}_{\mathcal{G}_r}$ itself. We conclude that with the comparison function $\beta(|s|_{\mathcal{G}_s})$, η_r is proven to be a (compact-set) ISS-Lyapunov function for the input s and the attractor $\mathcal{Z}_{\mathcal{G}_r}$. ■

IV. APPLICATION OF THE CONSTRUCTION

In these examples, the configuration space is the Euclidean plane \mathbb{R}^2 , and thus vector spaces \mathcal{R} , \mathcal{S} and \mathcal{Q} are all copies of \mathbb{R}^2 . Denote by \mathbf{J} the antisymmetric matrix $\begin{bmatrix} 0 & -1 \\ 1 & 0 \end{bmatrix}$, and (by abuse of notation) define a matrix valued $\mathbf{J}(x, y) := \begin{bmatrix} x & -y \\ y & x \end{bmatrix}$ that takes each point $(x, y) \in \mathcal{Q}$ to an orthogonal basis whose first vector is $(x, y)^T$. A useful constituent in the constructions to follow is the function $\mu(p) := (\{p + \alpha^2\})^{\frac{1}{2}}$, where α is a non-zero scale parameter to be selected.

1) *Reference Generator*: The reference (6) must be ISS with respect to the input s coupled via $v(\cdot, \cdot)$, and with respect to a compact goal \mathcal{G}_r . We would like the replanner to backtrack along the most recent motions of the plant and then try to move around the obstacle, and therefore maneuvers should act in a direction opposite to the most recent motion. If we assume that tracking error is small, the most recent motion would have been in the direction of $f(r)$. We therefore coupled the maneuver into the reference taking the direction of the reference vector field as the first axis

$$v(r, s) := \frac{c_{sr}}{\mu(f^T f)} \mathbf{J}(f) s. \quad (16)$$

The function $\mu(\cdot)$ satisfies $\mu(p^2) \geq p$, giving $\mu(f^T f) \geq \|\mathbf{J}(f)\|$ and thus $|v(r, s)| \leq c_{sr}|s|$, satisfying requirement (2b). Given a smooth Lyapunov function $\phi_r(r)$ for the system $\dot{r} = f(r)$, there exists a comparison function $\xi \in \mathcal{K}_\infty$ such that $\nabla\phi_r(r) \cdot f \leq -\xi(|r|_{\mathcal{G}_r})$, and using the same comparison function

$$\nabla\phi_r(r) \cdot (f + v) \leq -\xi(|r|_{\mathcal{G}_r}) + c_{sr}|s|, \quad (17)$$

establishing that $\phi_r(r)$ is an ISS-Lyapunov function for the system (6) as per requirement (2a).

a) *Point attractor reference system*: One of the reference systems we study below models a ‘‘flowbox’’ – a region of a vector field that is constant, or nearly so, by virtue of being en-route to a distant point attractor.. We take as our attractor the point $r_0 := (1000, 0)^T$, and define our Lyapunov function $\phi_r(r) := \mu(r^T \begin{bmatrix} 1 & 0 \\ 0 & 0.01 \end{bmatrix} r)$. Our reference system is chosen to be $f(r) := \nabla\phi_r(r)$, giving what is effectively a flowbox in the region $r_x < 0$. Our choice of ϕ_r is asymptotically linear in $|r|_{\mathcal{G}_r}$, causing f to satisfy requirement (2c).

b) *Saturated Hopf oscillator reference system*: The second reference system we examine models recurrent tasks, which may encounter a persistent disturbance multiple times. This reference is defined in terms of $\phi_r(r) := (|r|^2 - R_0^2)^2 / \mu(|r|^3)$, with the constant α of the saturation function set so that $\alpha^3 \gg R_0^4$, and thus the dynamics near the R_0 radius disc are close to those of the unsaturated system, while the linear asymptotic growth ensures that $\nabla\phi_r(r)$ is bounded. The state space is $\mathcal{Q} := \mathbb{R}^2 - \{0\}$, and the reference dynamics on this space are given by $f(r) := \nabla\phi_r(r) + \omega_0 \mathbf{J}r / \mu(r^T r)$, generating a constant angular rotation rate ω_0 in combination with the Hopf oscillator-like convergence to the circle at radius R_0 and also satisfying requirement (2c).

2) *ISS Replanner*: The replanning vector field g is a stable focus [27]:

$$g(s) := -k_g (\mathbf{I} + w_s \mathbf{J}) s \quad (18)$$

where scalar gain k_g adjusts the recovery rate from any perturbation on the transient dynamics, and the gain w_s adjusts the rate of rotation as expressed in the imaginary part of the eigenvalues. We excite maneuvers along the first coordinate of \mathcal{S} , driven by the magnitude of tracking error

$$u(e) := |e| / \mu(e^T e) \begin{bmatrix} 1 & 0 \end{bmatrix}^T \quad (19)$$

where $|u| < 1$ from $\mu(p^2) > p$, providing requirement (2d).

Let $\phi_s(s) := \mu(s^T s)$, giving $\nabla\phi_s(s) = s\mu'(s^T s)$. This gradient’s norm monotonically grows to 1 as $|s|$ grows to infinity. The Lie derivative $\dot{\phi}_s(s, e)$ of ϕ_s in the system (7) given by $\dot{s} = g(s) + u(e)$ is

$$\dot{\phi}_s(s, e) = \frac{g(s) \cdot s + u(e) \cdot s}{\mu(s^T s)} \leq \frac{|e|}{2\alpha} - \frac{k_g |s|}{2} \quad (20)$$

From [25] eqn. (7), ϕ_s is an ISS-Lyapunov function for the replanner, (7) is ISS with respect to attractor 0 and input e , and requirement (3) is satisfied².

3) *Integral-ISS Tracking Error Dynamics*: We implement a simple potential-dissipative

[16, 28] tracking controller (in this case, a generalized spring-damper) with saturated terms in a fashion similar to described in Appendix A, where $\phi_e(e) = k_e \mu(e^T e)$ and

$$E(e, \dot{e}) := -\nabla\phi_e(e) - \frac{m_e}{\mu(\dot{e}^T \dot{e})} \dot{e} \quad (21)$$

Proposition 3: $\ddot{e} = E(e, \dot{e})$ is GAS.

Proof: Consider the function

$$\eta_e := \phi_e(e) + \frac{1}{2} \dot{e}^T \dot{e} \quad (22)$$

$$\dot{\eta}_e = \nabla\phi_e(e) \cdot \dot{e} + \dot{e} \cdot \ddot{e} = -m_e \mu'(\dot{e}^T \dot{e}) |\dot{e}|^2 \leq 0 \quad (23)$$

For $\dot{e} = 0$ we note that $\ddot{e} = -\nabla\phi_e(e)$, and thus $(\ddot{e} \cdot e)|_{\dot{e}=0} < 0$, satisfying LaSalle’s condition and therefore ensuring that $\eta_e \rightarrow 0$. ■

Proposition 4: $\ddot{e} = E(e, \dot{e}) + d$ is iISS with respect to the attractor 0 and the input d .

Proof: We show that η_e of (22) satisfies the conditions of an iISS storage function, as per [18] equation (11).

$$\dot{\eta}_e = \frac{m_e}{\mu(\dot{e}^T \dot{e})} (\dot{e} \cdot d - \dot{e}^T \dot{e}) < \frac{m_e}{\mu(\dot{e}^T \dot{e})} |\dot{e}| |d| \quad (24)$$

By construction $\mu(x^2) > \max(x, \alpha)$, and thus $M := \sup\{x / \mu(x^2) | x \in \mathbb{R}_{>0}\}$ is finite. We may choose for [18] equation (11) to have $\sigma(|d|) := M|d|$. As we have already shown 0-GAS, the requirements of [18] theorem 1 case 4 are met, satisfying our design requirement (4). ■

²Note that we have formulated our theory allowing the replanner’s attractor to be a general compact set, rather than zero; this allows for ‘‘memory’’ – the maneuver state within the attractor can persist between excitations.

4) *Disturbance*: We model persistent disturbances by taking $d := \nabla h(q)$ for a scalar function h defined in terms of manually placed square tiles. This height-like disturbance potential h will be referred to as the “terrain”, although the magnitudes were chosen such that the terrain obstacles could not be surmounted with the force available to the controller. Each tile is endowed with a cubic mapping height from a displacement measured either radially from a corner or as a Cartesian distance from one of the edges of the tile. This collection of tiles allows the construction of C^2 smooth terrains, by appropriate selection of neighboring tiles; all simulated terrains are smooth.

V. SIMULATION STUDIES

A. Simulations and Quality Metrics

The controller architecture we propose lies on a continuum determined by the coupling gain c_{sr} of (16), at one end of which $c_{sr} = 0$ and the system simplifies to a classical trajectory tracker with the trajectory starting at $r(0)$ as its reference. As c_{sr} grows, maneuvers induced in s have larger effects on r . We demonstrate that for our example systems, an interval of c_{sr} values provides noticeably better system performance by several quality metrics: (1) tracking quality as represented by the Lyapunov function $\eta_{total} := \eta_r + \eta_e + \phi_s$; (2) reference convergence as represented by the Lyapunov function of the reference ϕ_r ; (3) power expenditure as expressed by the integral $E_{total} := \int |\ddot{q} \cdot \dot{q}| dt$. For the point attractor example, this integral is taken until the state variable q_x lies to the right of the terrain obstacle. For the Hopf examples, the integral is normalized by dividing by the number of rotations around the origin.

As can be observed in the accompanying figures, the proposed architecture results in considerable perturbation away from the trajectories of the undisturbed reference generator. Indeed, as discussed above, these deformations cannot be claimed optimal in any sense. Rather, they are feasible courses of action that respect the plant’s power and energy limitations.

All simulations were integrated using code derived from the `dopri5` code from [29], with the output interfaced to the SciPy open-source scientific Python environment³.

B. Point Attractor with comb obstacle

The first example shows the interaction of our controller with a “comb” obstacle punctuated by regularly spaced cul-de-sac traps (Figure 1), and demonstrates the how c_{sr} relates performance to the geometry of obstacles. Success at this task constitutes reaching a state with q_x to the right of the obstacle. The change in total energy consumption with varying c_{sr} is presented in Figure 2, and shows that while the interval $3.9 < c_{sr} < 18.0$ provides good performance, at larger values repeated resonance-like bands of degraded

performance appear (e.g. at $c_{sr} = 99.0$). Apparently these bands correspond to maneuver spatial scales that take the state out of one trap into another.

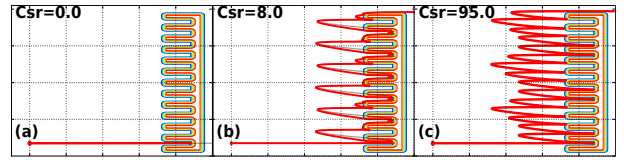


Fig. 1: Plant evolution for the point attractor reference meeting a comb obstacle with different transient to reference (c_{sr}) coupling gains((red) plant, (black) reference).

(a) For a small value of c_{sr} the particle remains blocked by the obstacle, (b) For a moderate c_{sr} value plant escapes with very low costs, (c),(d) For higher values of c_{sr} energy cost grows again with resonance peaks when the replanner induces escape maneuvers whose spatial frequencies couple strongly to the geometric features of the particular obstacle.

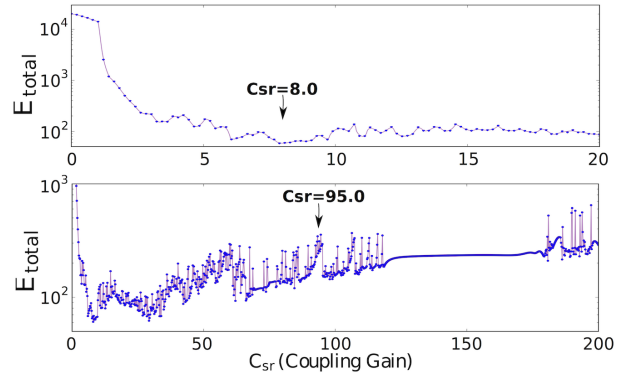


Fig. 2: Energy consumed over the course of the point attractor reference with comb obstacle depicted in Fig. 1 as a function of the transient to reference coupling gain, c_{sr} (of (16)). (a) Magnified view of small values of c_{sr} ; (b) Larger values of c_{sr} showing optimum, an approximately linear increase in cost with increased c_{sr} , and occasional resonance peaks where cost is larger over a narrow range.

C. Hopf reference with two obstacles

In these two examples, the task encoded by the reference system continually brings the plant back into interaction with an obstacle that blocks the limit cycle, and includes a trap that would completely block a simple reference tracker.

For both the simple obstacle A (Figure 3) and the more elaborate obstacle B (Figure 4), our controller manages to escape the traps. For a range of c_{sr} values, the system then exhibits a modified cycle which accomplishes the task with moderate energy consumption (Figure 5 obstacle A; Figure 6 B).

From the point of view of iISS theory, it should be noted that in these simulations $\|d\|_2$ is unbounded since the obstacle interaction has support in every cycle. Thus we can not expect convergence to \mathcal{G}_r , nor should we anticipate η_{total} and ϕ_r to go to zero (see Figure 7).

³Scientific Tools for Python, www.scipy.org. Using our code this provided an extremely fast ODE integrator. In our tests it gave $1.02 \cdot 10^6$ trajectory points a second of a Rossler system’s chaotic orbit on a single core of an Intel i5 CPU at 2.67 GHz – an order of magnitude faster than the commonly used MatLab `ode45` integrator on the same platform.

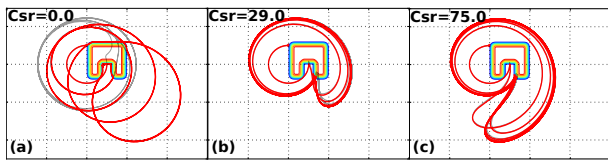


Fig. 3: Plant evolution for the Hopf cycle attractor reference meeting a simple obstacle with different transient to reference coupling gains (red plant, black reference). (a) Classical trajectory tracker (Zero or small c_{sr}) gets trapped until the reference sweeps back behind it – at which point it is pulled out and proceeds to cycle hitting the obstacle again at a different position, effectively trapped in place. (b) At a sufficiently large c_{sr} a qualitative change appears – the plant hits the obstacle exactly once every cycle and then back-tracks and circles the obstacle, achieving a deformation on the reference trajectory cycle. (c) At even larger c_{sr} this regular trajectory deforms more and more.

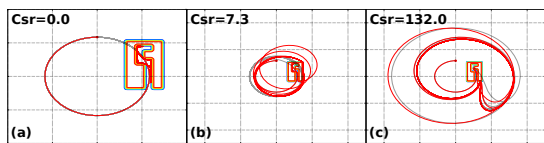


Fig. 4: Plant evolution for the Hopf cycle attractor reference meeting an elaborate obstacle with different transient to reference coupling gains (red plant, black reference). (a) The classical trajectory tracker (small or zero c_{sr}) gets trapped in the cul-de-sac as expected, and unlike the previous case, even though the reference trajectory gets behind the plant at each period, the plant can not leave the trap. (b),(c) At a sufficiently large c_{sr} a qualitative change appears whereby the initial hit excites a successful escape recovery trajectory which returns along the unblocked portion of the cycle to repeat the same pattern, cycle after cycle.

VI. CONCLUSION

In this study we introduce a novel reference generator and tracking control architecture that enjoys appropriate stability properties and we present a handful of simulations demonstrating its ability to dislodge a simple point mass particle from cul-de-sac traps that block a naive tracking controller. The energy costs calculated over a range of controller gains exhibit similar features for all three systems: a minimal threshold for escaping the trap, followed by a small range over which energy cost fluctuates, then a “sweet spot” exhibiting qualitatively “best” behavior that extends over a significant interval, followed by a roughly linear increase, and finally a more-or-less linear increase in cost, with many irregular cost fluctuations.

A key feature of this architecture lies in its ability to isolate task specification – the reference subsystem (9) – from the “replanner” (7) – the encoding of how to handle unanticipated but structured obstacles to its execution.

In contrast to the traditions of adaptive control (where disturbance structure is specified in advance up to unknown parameters) or robust control (where disturbance structure is specified by an appropriately delimited region of function space) it is not clear to us at present how to formalize

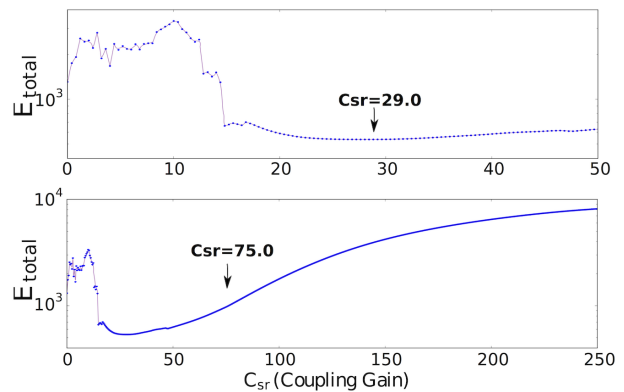


Fig. 5: Energy consumed over the course of the Hopf cycle attractor reference with simple obstacle depicted in Fig. 3 as a function of the transient to reference coupling gain. (a) Magnified view of small values of c_{sr} ; (b) Larger values of c_{sr} showing optimum, an approximately linear increase in cost with increased c_{sr} , and occasional resonance peaks where cost is larger over a narrow range.

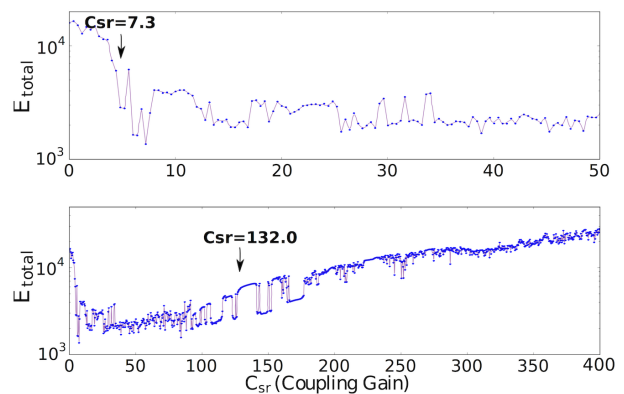


Fig. 6: Energy consumed over the course of the Hopf cycle attractor reference with elaborate obstacle depicted in Fig. 4 as a function of the transient to reference coupling gain. (a) Magnified view of small values of c_{sr} ; (b) Larger values of c_{sr} showing optimum, an approximately linear increase in cost with increased c_{sr} , and occasional resonance peaks where cost is larger over a narrow range.

the sort of “unanticipated but structured” disturbances best handled by this architecture. Still less is it clear how to then exploit that structure, e.g. via more methodical or perhaps even “optimal” constructions of the replanner dynamics (7). However, we believe that a wide range of disturbances in realistic settings display the character of “blind obstacles” in the state space that here we instantiate literally in a hypothetical particle configuration space. This literal setting underscores the intuitive wisdom of the transient system we have implemented: its ability to backtrack relative to the reference vector field, and to move laterally, allowing it to escape various traps at moderate energetic cost. Such useful notions as “replanning” and “backtracking” have long remained the exclusive province of AI [30], and we hope that the present effort to bring these ideas into the fold of control theory might be enriching to both fields.

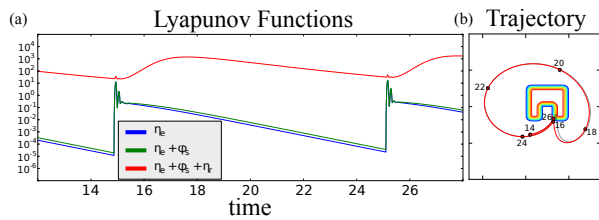


Fig. 7: Contributions to total Lyapunov function η_{total} for one cycle of the Hopf system. The tracking error Lyapunov η_e (red) comprising potential (cyan) and kinetic terms grows rapidly when the obstacle is hit, causing a growth of the transient ϕ_s ($\eta_e + \phi_s$ in green). The ISS Lyapunov function η_{total} (blue) continues to grow until the transient becomes sufficiently small, and then it too decays exponentially.

ACKNOWLEDGEMENTS

This work was supported in part by AFOSR under the CHASE MURI FA95501010567 and in part by ONR under the HUNT MURI N00014-07-0829.. The authors would like to thank M. S. Berns for her contribution to preliminary stages of this work, and J. M. Guckenheimer for providing the numerical integration codes on which the simulations were based.

REFERENCES

- [1] M. Buehler, D. E. Koditschek, and P. J. Kindlmann, "Planning and control of robotic juggling and catching tasks," *International Journal of Robotics Research*, vol. 13, no. 12, pp. 101–118, April 1994.
- [2] A. A. R. Rizzi and D. E. Koditschek, "An active visual estimator for dexterous manipulation," *IEEE Transactions on Robotics and Automation*, vol. 12, no. 5, pp. 697–713, Oct 1996.
- [3] J. Nakanishi, T. Fukuda, and D. E. Koditschek, "A brachiating robot controller," *Robotics and Automation, IEEE Transactions on*, vol. 16, no. 2, pp. 109–123, 2000.
- [4] G. A. Lynch, J. E. Clark, and D. E. Koditschek, "A self-exciting controller for high-speed vertical running," in *International Conference on Intelligent Robots and Systems*, St. Louis, Missouri, USA, October 2009.
- [5] U. Saranlı, M. Buehler, and D. E. Koditschek, "RHEx: a simple and highly mobile hexapod robot," *The International Journal of Robotics Research*, vol. 20, no. 7, p. 616, 2001.
- [6] E. R. Westervelt, J. W. Grizzle, and D. E. Koditschek, "Hybrid zero dynamics of planar biped walkers," *IEEE Transactions on Automatic Control*, vol. 48, no. 1, pp. 42–56, 2003.
- [7] M. J. Spenko, J. A. Saunders, G. C. Haynes, M. R. Cutkosky, A. A. Rizzi, R. J. Full, and D. E. Koditschek, "Biologically inspired climbing with a hexapedal robot," *Journal of Field Robotics*, vol. 25, no. 4-5, pp. 223–242, 2008.
- [8] D. E. Koditschek, "Adaptive techniques for mechanical systems," in *Proc. 5th. Yale Workshop on Adaptive*

Systems, May 1987, pp. 259–265. [Online]. Available: http://repository.upenn.edu/ese_papers/416/

- [9] H. Choset, K. M. Lynch, S. Hutchinson, G. Kantor, W. Burgard, L. Kavraki, and S. Thrun, *Principles of robot motion: theory, algorithms, and implementations*. MIT Press, Cambridge, MA, 2005.
- [10] A. De, G. Lynch, A. Johnson, and D. Koditschek, "Motor sizing for legged robots using dynamic task specification," in *Technologies for Practical Robot Applications (TePRA), 2011 IEEE Conference on*, 2011, p. 6469.
- [11] S. Tarbouriech and M. Turner, "Anti-windup design: an overview of some recent advances and open problems," *IET Control Theory & Applications*, vol. 3, no. 1, p. 119, Jan 2009.
- [12] E. Gilbert and I. Kolmanovsky, "Nonlinear tracking control in the presence of state and control constraints: a generalized reference governor," *Automatica*, vol. 38, no. 12, p. 20632073, 2002.
- [13] E. D. Sontag, *Input to state stability: Basic concepts and results*, ser. Lecture Notes in Mathematics. Springer Verlag, 2008, vol. 1932.
- [14] F. Blanchini and S. Miani, "Constrained stabilization via smooth lyapunov functions," *Systems & control letters*, vol. 35, no. 3, p. 155163, 1998.
- [15] F. Morabito, A. R. Teel, and L. Zaccarian, "Nonlinear antiwindup applied to euler-lagrange systems," *IEEE Transactions on Robotics and Automation*, vol. 20, no. 3, p. 526 537, Jun 2004.
- [16] D. E. Koditschek, *The application of total energy as a Lyapunov function for mechanical control systems*. AMS, 1989, vol. 97, p. 131157.
- [17] E. D. Sontag, *The ISS philosophy as a unifying framework for stability-like behavior*, 2000, pp. 443–468.
- [18] D. Angeli, E. Sontag, and Y. Wang, "A characterization of integral input-to-state stability," *IEEE Trans Autom Control*, vol. 45, no. 6, pp. 1082–1097, JUN 2000.
- [19] D. E. Koditschek, "Task encoding: toward a scientific paradigm for robot planning and control," *Robotics and autonomous systems*, vol. 9, no. 1-2, pp. 5–39, 1992.
- [20] E. Rimon and D. E. Koditschek, "Robot navigation functions on manifolds with boundary," *Advances in Applied Mathematics*, vol. 11, pp. 412–442, 1990.
- [21] N. Ayanian, V. Kallem, and V. Kumar, "Synthesis of feedback controllers for multiple aerial robots with geometric constraints," in *Proc. IEEE/RSJ Int. Conf. Intell. Robots Syst.*, 2011, p. (in press).
- [22] A. A. Rizzi, "Hybrid control as a method for robot motion programming," in *Robotics and Automation, 1998. Proceedings. 1998 IEEE International Conference on*, vol. 1, 1998, p. 832837.
- [23] D. C. Conner, H. Choset, and A. A. Rizzi, "Flow-through policies for hybrid controller synthesis applied to fully actuated systems," *Robotics, IEEE Transactions on*, vol. 25, no. 1, p. 136146, 2009.
- [24] J. D. Weingarten, R. E. Groff, and D. E. Koditschek, "A framework for the coordination of legged robot gaits,"

in *Robotics, Automation and Mechatronics, 2004 IEEE Conference on*, vol. 2, 2004.

- [25] E. D. Sontag and Y. Wang, "On characterizations of input-to-state stability with respect to compact sets," in *Proc. IFAC Non-Linear Control Systems Design Symposium (NOLCOS '95)*, 1995, pp. 226–231.
- [26] D. Liberzon, E. Sontag, and Y. Wang, "Universal construction of feedback laws achieving iss and integral-iss disturbance attenuation," *Systems & Control Letters*, vol. 46, no. 2, pp. 111–127, 2002. [Online]. Available: <http://www.sciencedirect.com/science/article/pii/S0167691102001251>
- [27] V. I. Arnold, *Ordinary Differential Equations*. MIT Press, 1973.
- [28] D. E. Koditschek, "The control of natural motion in mechanical systems," *Journal of Dynamic Systems, Measurement, and Control*, vol. 113, p. 547551, 1991.
- [29] E. Hairer, S. P. Nørsett, and G. Wanner, *Solving Ordinary Differential Equations I, Nonstiff Problems*, 2nd ed., ser. Springer Series in Computational Mathematics. Springer, 2008, vol. publisher.
- [30] S. Russell and P. Norvig, *Artificial Intelligence: A Modern Approach*. Prentice Hall Upper Saddle River, NJ, 2010.

APPENDIX

A. Saturating a Quadratic Form

A canonical example of a stable system is the gradient of a quadratic potential well. If we wish to produce a system whose dynamics next to the origin are those of a quadratic potential well, but whose asymptotic growth at infinity is chosen arbitrarily, it is convenient to use a radial rescaling of a quadratic form, and use its gradient. As we feel this construction is of general utility, we provide a general derivation, followed by a specialization to the case used in our examples.

B. Radially rescaled quadratic potentials

Let ϕ_x be defined as:

$$\phi_x(x) := \Psi(x^T M x) \quad (25)$$

where $\Psi : \mathbb{R}^+ \rightarrow \mathbb{R}^+$ is C^1 and monotone, and M is symmetric and positive. The Gradient and Hessian of this function can be derived as:

$$\nabla \phi_x x = 2\Psi' M x \quad (26)$$

$$H_{\phi_x}(x) = 4\Psi'' M x x^T M + 2\Psi' M \quad (27)$$

where Ψ' and Ψ'' are first and second derivatives of Ψ evaluated at $x^T M x$.

C. Saturated gradients at infinity

Let us now further specialize, by choosing the saturation function Ψ to be $\mu(\cdot)$:

$$\mu(p) := (p + \alpha^2)^{\frac{1}{2}} \quad (28)$$

$$\mu'(p) = \frac{1}{2} (p + \alpha^2)^{-\frac{1}{2}} = \frac{p}{2\mu(p)} \quad (29)$$

$$\mu''(p) = -\frac{1}{4} (p + \alpha^2)^{-\frac{3}{2}} = -\frac{p}{4(\mu(p))^3} \quad (30)$$

which leads to:

$$\phi_x(x) = (x^T M x + \alpha^2)^{\frac{1}{2}} \quad (31)$$

$$\nabla \phi_x(x) = \frac{M x}{\phi_x(x)} \quad (32)$$

$$H_{\phi_x}(x) = \frac{M}{\phi_x(x)} - \frac{M x x^T M}{(\phi_x(x))^3} \quad (33)$$

D. The gradient is bounded

Take $\gamma > 0$ to be the minimal eigenvalue of M , and $\|M\|$ the operator norm of M . These provide tight bounds $\|M\| |x| \geq |M x| \geq \gamma |x|$, from which we may obtain

$$\frac{\gamma^2 |x|^2}{\|M\| |x|^2 + \alpha^2} \leq |\nabla \phi_x(x)|^2 \leq \frac{\|M\|^2 |x|^2}{\gamma |x|^2 + \alpha^2} \quad (34)$$

and thus for any $\varepsilon > 0$ a sufficiently large $|x|$ provides

$$\gamma \|M\|^{-\frac{1}{2}} - \varepsilon \leq |\nabla \phi_x(x)| \leq \|M\| \gamma^{-\frac{1}{2}} + \varepsilon \quad (35)$$

E. The Hessian can be made positive

The Hessian in (33) is a rational function of the matrix M , and must therefore share eigenvectors with M .

Let \bar{x} be a unit eigenvector of M with eigenvalue λ . To show positivity of $H_{\phi_x}(x)$, it is enough to show that for all x , $\bar{x}^T H_{\phi_x}(x) \bar{x} > 0$:

$$\begin{aligned} \bar{x}^T H_{\phi_x}(x) \bar{x} &= \frac{1}{\phi_x(x)} \left(\bar{x}^T M \bar{x} - \left(\frac{\bar{x}^T M x}{\phi_x(x)} \right)^2 \right) \\ &= \frac{\lambda}{\phi_x(x)} \left(1 - \frac{\bar{x} \cdot x}{x^T M x + \alpha^2} \right) \\ &> \frac{\lambda}{\phi_x(x)} \left(1 - \frac{|x|}{\gamma |x|^2 + \alpha^2} \right) \end{aligned} \quad (36)$$

If our system is chosen such that $\gamma > \frac{1}{4\alpha^2}$, then the quadratic $\gamma |x|^2 - |x| + \alpha^2 = 0$ has no real solutions and therefore the Hessian is positive definite everywhere.